Spin–orbit-coupling effects on *g*-value and damping factor of the ferromagnetic resonance in Co and Fe films

2003 J. Phys.: Condens. Matter 15 S451

(http://iopscience.iop.org/0953-8984/15/5/302)

INSTITUTE OF PHYSICS PUBLISHING JOURNAL OF PHYSICS: CONDENSED MATTER

J. Phys.: Condens. Matter **15** (2003) S451–S463 PII: S0953-8984(03)55328-0

Spin–orbit-coupling effects on g-value and damping factor of the ferromagnetic resonance in Co and Fe films

J Pelzl[1], R Meckenstock[1], D Spoddig[1], F Schreiber[1,3], J Pflaum[1,4] and Z Frait[2]

[1] Institut für Experimentalphysik, AG Festkörperspektroskopie, Ruhr-Universität, D-44801 Bochum, Germany
[2] Institute of Physics, Academy of Science, Praha 8, CZ

Received 29 October 2002
Published 27 January 2003
Online at stacks.iop.org/JPhysCM/15/S451

Abstract

The spectroscopic splitting factor g and the Gilbert damping constant G are magnetic parameters accessible to ferromagnetic resonance (FMR) measurements, which apart from the magneto-crystalline anisotropy energy can provide information on the spin–orbit coupling in magnetically ordered material. Whereas the effect of spin–orbit coupling has been thoroughly investigated and is well understood in insulating transition metal compounds, in 3d-metallic magnetic compounds the microscopic mechanism still needs further clarification. Particularly in thin films and multilayers interface effects and interaction between layers can modify both spin and orbital moments leading to changes of the g-value and the Gilbert damping constant. Experimental results are presented from frequency dependent FMR measurements on Co epitaxial films grown on Cr(001) and on films of the alloy $Co_{1-x}Fe_x(100)$ deposited on MgO(001), and from recent studies on Fe(100) films grown on InAs(001). The experimental data yield clear evidence of the importance of surfaces or interfaces of the films on the magnitude of orbital and spin moment.

(Some figures in this article are in colour only in the electronic version)

1. Introduction

The magnetic resonance spectroscopy in the microwave range relies on the transition between the Zeeman components of the electronic levels. The splitting at a given external magnetic field yields direct information on the magnetic moment of the atoms or ions involved in the resonance transition. Spin and orbit contribute to the total moment. The magnitude of the

[3] Present address: University of Oxford, Physical and Theoretical Chemistry Laboratory, South Parks Road, Oxford OX13QZ, UK.
[4] Present address: Universität Stuttgart, 3. Physikalische Institut, Pfaffenwaldring 57, D-70569 Stuttgart, Germany.

orbital part and its contribution relative to the total moment are governed by the spin–orbit interaction in competition with the electrostatic interactions between the electrons themselves and between the electrons and the surrounding charges. For 3d elements the problem has been thoroughly investigated for the ground state of free ions and also for these ions in insulating compounds (Abragam and Bleany 1970, Pake 1962). A characteristic feature of the 3d transition ion compounds is the quenching of the orbital momentum by the strong crystalline field. Therefore the g-factor of the ground state is close to the value of the free electron. The spin–orbit coupling is smaller by roughly one order of magnitude compared to 4f elements and can be treated as perturbation mixing of the eigenstates of crystalline field split levels. Therefore the deviation of the g-factor from the free electron value is proportional to λ_{SO}/Δ where λ_{SO} and Δ are the spin–orbit coupling parameter and the ground state–first excited state splitting of the corresponding 3d ion. As λ_{SO} can be positive or negative the g-factor can be smaller or larger than two. In addition, due to the higher order mixing of orbital contributions to the ground state by the spin–orbit coupling the symmetry of the surrounding crystal field is impressed and the g-factor becomes dependent on the orientation of the external magnetic field with respect to the crystalline symmetry axes. Therefore the g-factor of 3d transition ions in insulating compounds has tensorial character with values of the principal axes depending on the site symmetry of the ion (Orton 1968).

In 3d-metallic magnetic compounds the overall conditions concerning the relative strength of the crystal field interaction and the spin–orbit coupling are in general very similar to those in the ionic compounds, but due to the itinerant character of the electrons the resultant effects have to be described in a band structure model. Magnetic resonance of the 3d elements is observed mostly in the magnetically ordered state where additional interaction fields resulting from exchange and dipolar coupling of the magnetic moments contribute to the splitting of the Zeeman levels. Therefore, the determination of the g-factor by the magnetic resonance in magnetically ordered compounds is more troublesome, requiring frequency dependent measurements (see the next paragraph). On the other hand, the measurement of the g-factor is apart from magnetic neutron scattering and magnetic x-ray dichroism the only experimental method offering access to the separation of the spin and orbital contributions to the total magnetic moment. Proceeding from the pioneering works of Kittel (1949) and Van Vleck (1950), Meyer and Asch (1961) and later Reck and Fry (1969) derived a relation between the g-factor of the magnetic resonance in ferromagnetic (FMR) compounds and the magnetization contributions due to spin and orbital angular momentum. For small orbital contributions the deviation from the spin g-factor of two is small and is given by

$$g - 2 = 2\left(\frac{\mu_L}{\mu_S}\right) \tag{1}$$

where μ_L and μ_S are the magnetic moments of the orbital and of the spin, respectively. Meyer and Asch (1961) and Reck and Fry (1969) investigated experimentally the orbital to spin ratio in bulk samples of 3d transition metals and alloys. For the alloys the authors made a thorough study of the variation of the spin and orbital contributions as a function of composition. Relation (1) is also applied in current research on thin metallic films to quantify the influence of the surface and interface effects on the orbital and spin contributions to the magnetic moment (Schreiber 1995, Anisimov *et al* 1999). A major part of this report is devoted to this aspect.

Theoretical studies of the spin–orbit-coupling effects in magnetic metals of 3d transition elements have been made only more recently (Daalderop *et al* 1995, Eriksson 2001). In the frame of band structure models the magnetic crystalline anisotropy energy has been calculated for Co layers and Co alloy layers. An analytical relation between anisotropy field and orbital

momentum due to the spin–orbit coupling has been proposed by Bruno (1989) but could not be confirmed by recent band structure calculations (Ujfalussy *et al* 1995).

Dynamical effects which are mediated by the spin–orbit coupling are the spin–lattice relaxation in paramagnetic compounds and the magnon–phonon scattering in magnetically ordered systems. The line width of the magnetic resonance provides a means to study experimentally both processes. For insulating paramagnetic compounds the relaxations of the spins have been investigated thoroughly in the past 30 years and commonly analysed on the basis of the Bloch equations (see e.g. Abragam and Bleany 1970). In the case of the FMR in magnetically ordered compounds Landau and Lifschitz (1935) and Gilbert (1955) introduced damping factors to describe the decay of the magnetization precession. For single layers or in the absence of interlayer exchange interaction the line width is directly proportional to these damping factors and increases linearly with the microwave frequency (see the next paragraph). The microscopic mechanisms contributing to the damping factors are still under investigation. The approach of Kambersky (1970) for magnetic metallic systems assumes two different processes for the relaxation of the net magnetization which he called the ordinary process and spin-flip process. The Gilbert damping factor G for both processes depends on the density of states at the Fermi level Z_F and on the electron scattering time τ and are directly proportional to the square of the deviation of the g-factor from its free spin-value.

$$\begin{aligned} &\text{Spin-flip scattering:} && G = (\gamma\hbar/2)^2 Z_F (g-2)^2/\tau \\ &\text{Ordinary scattering:} && G = (\gamma/2)^2 Z_F \lambda_{SO}^2 (g-2)^2 \tau. \end{aligned} \tag{2}$$

Here λ_{SO} is the spin–orbit-coupling constant. With regard to equation (1) it should be noticed that the damping factor varies with the square of the ratio of the orbital to spin moment. Therefore, the G-factor provides a very sensitive probe for the spin–orbit-coupling effects providing an indication of whether the g-factor shift is due mainly to the spin–orbit coupling. To deduce the damping factor from the line width and to determine the g-factor with high accuracy FMR measurements as a function of the microwave frequency are required.

In this contribution we review recent studies of the g-factor and damping factor G of the FMR in order to elucidate spin–orbit-effects in 3d-metallic films. Particularly in thin films and multilayers interface effects and interaction between layers can modify both spin and orbital moments leading to changes of the g-value and the Gilbert damping constant. We show that depending on the sample these effects can be induced by compositional changes, by interface interactions or by lattice relaxation. After a brief description of the FMR signal in mono-domain epitaxial films in the following chapter experimental results will be presented from frequency dependent FMR measurements on Co epitaxial films grown on Cr(001), and on films of the alloy $Co_{1-x}Fe_x(100)$ deposited on MgO and of recent studies on Fe(100) films grown on InAs. Although emphasis is put on the study of g-factor and damping factor G systematic trends observed in the crystalline anisotropy constants will also be analysed and discussed in view of the behaviour of the spectroscopic parameters g and G.

2. The FMR signal from thin magnetic films

FMR describes the resonant absorption of microwaves which matches the Zeeman splitting of the energy levels in a ferromagnetic material. In a classical picture the magnetization precesses around the direction of an effective static magnetic field composed of the external field and the intrinsic fields described below. The precession described by the equation of motion given by Landau and Lifschitz (1935) and the damping term formulated by Gilbert (1955) leads to

$$\frac{\mathrm{d}\vec{M}}{\mathrm{d}t} = -\gamma(\vec{M} \times \vec{B}_{eff}) + \frac{\alpha}{M}\left(\vec{M} \times \frac{\mathrm{d}\vec{M}}{\mathrm{d}t}\right) \tag{3}$$

where M is the saturation magnetization, α is the dimensionless damping parameter, γ is the gyro-magnetic ratio defined as $\gamma = g\mu_B/\hbar$ and μ_B is the Bohr magneton. The damping parameter α in the SI system is related to the commonly used Gilbert damping factor G in CGS units by the equation

$$\alpha = G4\pi/\mu_0 M\gamma. \tag{4}$$

The different contributions to B_{eff} like anisotropy fields and exchange fields are taken into consideration by the free energy density via the relation

$$\mathrm{d}F = \vec{B}_{eff} \cdot \mathrm{d}\vec{M}. \tag{5}$$

For thin magnetic films and superlattices the free energy density functional F has to comprise the following major contributions:

$$F = F_{Zee} + F_{dem} + F_{ani} + F_{coupl}. \tag{6}$$

The Zeeman term describes the energy contribution of the external magnetic field: $(-\vec{M}\cdot\vec{B}_{ext})$. The demagnetizing term is given by $(\vec{M} \cdot \underline{\underline{N}}\mu_0\vec{M})$. In the case of a thin film with strongly reduced third dimension one has to consider only the N_{zz} component. The anisotropy part of the free energy depends on the crystalline structure of the investigated films and is mainly caused by the spin–orbit coupling. Terms like crystalline anisotropy, surface anisotropy and strain anisotropy needed for a comprehensive description of the magnetic behaviour of films like hcp Co, fcc FeCo or bcc Fe are given in the respective parts of this paper.

To describe the position and the line width of the FMR field and to consider the symmetry of the given lattice it is useful to change to polar coordinates. Therefore the Landau–Lifshitz equation is transformed to a coordinate system precessing at the top of the magnetization vector. One gets the dispersion law of the equation of motion described e.g. in Vonsovskii (1960):

$$\left(\frac{\omega}{\gamma}\right)^2 = \frac{1+\alpha^2}{M^2\sin^2(\Theta)}\left[\frac{\partial^2 F}{\partial\Theta^2}\frac{\partial^2 F}{\partial\Phi^2} - \left(\frac{\partial^2 F}{\partial\Theta\partial\Phi}\right)^2\right] \tag{7a}$$

with the equilibrium conditions

$$\frac{\partial F}{\partial\Theta} \stackrel{!}{=} 0; \qquad \frac{\partial F}{\partial\Phi} \stackrel{!}{=} 0 \tag{7b}$$

with Θ and Φ as polar and azimuthal angles.

The important point for the derivation of equation (7*a*) is that it is developed by perturbation expansion. The magnitude of the magnetization vector is considered constant with only a small shift away from its equilibrium position. For the resonance experiments this means that the amplitude of the microwave field in the cavity should not be too high to fulfil this assumption. Within the same derivation one finds for the line width (e.g. Vonsovskii 1960)

$$\Delta\omega = \frac{\gamma\alpha}{M}\left(\frac{\partial^2 F}{\partial\Theta^2} + \frac{1}{\sin^2(\Theta)}\frac{\partial^2 F}{\partial\Phi^2}\right); \qquad \Delta B = \frac{\partial B}{\partial\omega}\Delta\omega \tag{8}$$

with $\Delta\omega$ the intrinsic frequency line width and ΔB the intrinsic field line width.

Including extrinsic influences like roughness or inhomogeneities the measured line width can be written for hard in-plane axes:

$$\Delta B = \Delta B_0 + 2\alpha\frac{\omega}{\gamma} \tag{9}$$

where ΔB_0 contains all extrinsic contributions. Thus, the damping parameter α can be deduced from the slope of the line width versus microwave frequency plot.

The resonance condition including the equilibrium conditions obtained from equation (7) can be written in the form

$$\omega^2 = \gamma^2 B^2 + a(M, K_1, K_u, \Phi)\gamma^2 B + b(M, K_1, K_u, \Phi)\gamma^2 \tag{10}$$

where the factors a and b are linearly dependent on the anisotropy constants K_1 and K_u and the saturation magnetization M and are a function of the angle Φ between the orientations of the external field and the crystal axes. From frequency dependent measurements one can derive the g-value from the linear first part of equation (10) where the anisotropy contributions are much smaller than the magnetic field B.

3. Experimental setups for angle and frequency dependent FMR

Angle dependent FMR measurements were performed with an electron paramagnetic resonance spectrometer in the X-band. The sample was rotated inside a microwave cavity with respect to the crystal axes. The angular resolution was better than 0.02°. The frequency dependent measurements have been carried out with a shorted waveguide setup. With high accuracy towards the crystal axes the sample was used as a part of the wall of the waveguide. Both spectrometers used a Varian electro-magnet with a maximum field of 2.5 T (respectively 3.3 T). The measurements in the X-band used an automatic frequency control (AFC) to adjust the change in cavity resonance frequency due to absorption during FMR and rotation of the sample. For the shorted waveguide setup an AFC was not necessary, because the adjustment has to be done before recording each spectrum.

4. Results and discussion

4.1. Compositional induced effects in CoFe on MgO(100)

The alloy system Fe_xCo_{1-x} is most interesting because of its composition dependence of both the structural and the magnetic properties. Bulk Fe has bcc structure and bulk Co possesses hcp structure. Sometimes epitaxial grown Co films can be also stabilized in fcc structure. Concerning the magnetic properties Fe_xCo_{1-x} at $x = 0.65$ represents that alloy which has the highest magnetization at room temperature. Roughly at the same composition in bulk samples the magneto-crystalline anisotropy K_1 vanishes in order to become negative at higher Co concentrations. This crossover from positive to negative K_1 is not only of interest for technical application of the alloy but should also have an impact on the g-factor and on the damping constant.

Epitaxial films of Fe_xCo_{1-x} at different compositions were grown on MgO(100) substrates by the RF-sputter technique (Mühge 1994). The typical thickness of the alloy layer was 20 nm. For the *ex situ* FMR measurements the layer was covered with a 4 nm gold layer. The chemical composition of the alloy film was estimated by energy dispersive x-ray analysis. The Co film ($x = 0$) exhibited the fcc-(001) phase with (100)-fcc axis parallel to MgO(100) which switches over in the bcc-(100) phase of Fe below the concentration of 80% Co ($x = 0.2$) where the bcc-(100) axis is oriented parallel to MgO(110). In-plane angle dependent FMR at room temperature at 9.2 GHz indicates a fourfold symmetry together with a small uniaxial contribution. The cubic anisotropy constant K_1 deduced from these measurements as a function of concentration varies from a positive Fe value on the Fe-rich side to a negative Co value on the Co-rich side (figure 1) (Pflaum 1995, Pflaum *et al* 1995).

The comparison of the cubic anisotropy constant of the film samples with those obtained for bulk samples indicates a shift of the crossover to higher Fe concentrations which is thickness dependent and will be discussed later.

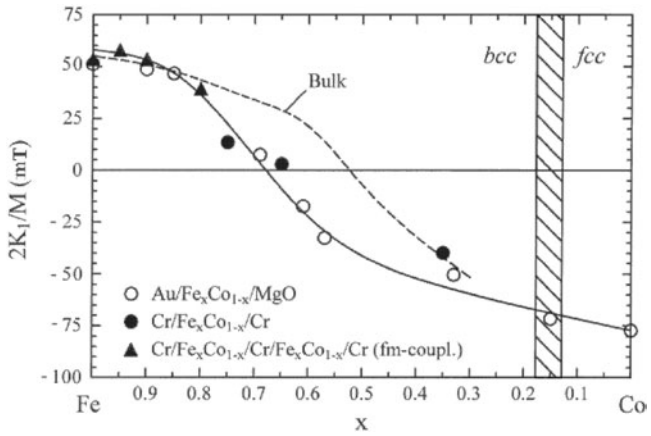

Figure 1. Concentration dependence of the magneto-crystalline anisotropy field $2K_1/M$ observed in Fe_xCo_{1-x} on different substrates. The dashed curve indicates the behaviour in the bulk alloy (Hall 1960).

The g-factor exhibits a quite different concentration dependence (figure 2). Particularly on the Fe-rich side up to $x = 0.5$ where the anisotropy K_1 and the effective magnetization (not shown here) vary distinctly, the g-factor remains constant at the value of bcc-iron which is $g = 2.085$. For fcc-cobalt $g = 2.145$ which corresponds to a reduction of the orbital contribution from 9% in hcp-Co to 7% in fcc-Co. This result stresses the importance of the site symmetry to the spin–orbit coupling effects. A theoretical approach for the concentration dependence of the g-factor had been proposed on the basis of weakly interacting sublattices (Tsuya 1952, Wangsness 1953). It is given by the relation

$$g(x) = \frac{x\mu_a + (1-x)\mu_b}{x\mu_a/g_a + (1-x)\mu_b/g_b} \tag{11}$$

where μ_a, g_a and μ_b, g_b are the magnetic moments and g-values of the two sublattices and are shown as the dashed curve in figure 2. The deviations from the experimental data particularly in the intermediate concentration range are considerable. To improve the theoretical model Schreiber and Pflaum modified the TW-theory by using concentration dependent values of Fe and Co moments (Schreiber 1995, Pflaum 1995, Schreiber *et al* 1995). Neither the original nor the modified theory can satisfactorily describe the measured concentration dependence. The origin of the peculiar concentration dependence remains unexplained. As the Gilbert damping factor behaves very similarly, band structure effects are most probably responsible for the observed deviation. Compositional inhomogeneities due to spatial variation of concentration can be ruled out on the basis of the line width data. The inhomogeneous contribution to the FMR line width increases monotonically with Co concentration without showing a maximum in the intermediate concentration range (Pflaum 1995).

The Gilbert damping factor G is obtained from the slope of the frequency variation of the peak to peak line width of the FMR signal. The frequency shift of the peak to peak line width ΔB_{PP} is composed of a homogeneous contribution proportional to G and an inhomogeneous contribution which is independent of the microwave frequency and is caused by the inhomogeneous local field distribution. This inhomogeneous part is larger for the magnetic field along the in-plane hard axis as compared to the easy axis and increases slightly (less than a factor of two) with increasing Co content. From the homogeneous or intrinsic part the G-factor has been determined according to relations (9) and (4) as a function of concentration (figure 3).

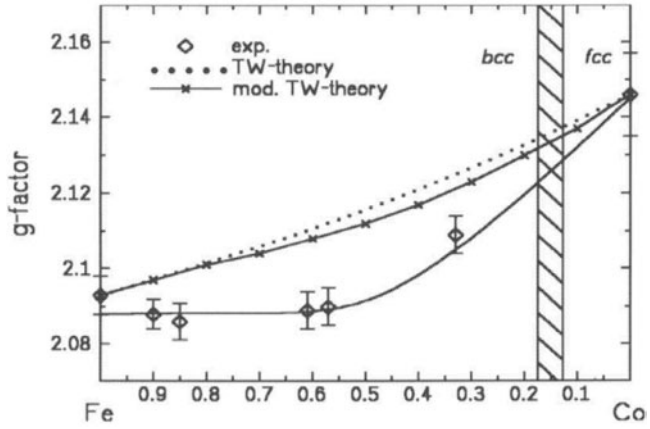

Figure 2. Concentration dependence of the g-factor of Fe_xCo_{1-x} at room temperature estimated by FMR compared with the original and modified theory of Tsuya and Wangsness.

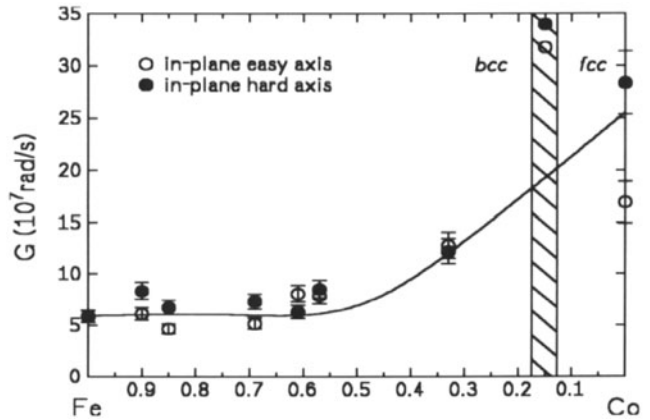

Figure 3. Concentration dependence of the Gilbert damping constant G in Fe_xCo_{1-x} at room temperature deduced from the intrinsic part of the peak to peak line width of the FMR.

Similar to the g-factor the damping factor is nearly constant in the iron-rich range. In the frame of the microscopic models of Kambersky, G should be proportional to $(g-2)^2$. A plot of G versus $(g-2)^2$ values for different compositions yields a reasonable straight line with a slope of 9×10^9 rad s^{-1}. Small deviations from the linear dependence should be expected due to the concentration dependence of the density of states near the Fermi level. Nevertheless, this result is the first experimental evidence of a direct relation between the g-factor and G damping constant in the frame of a spin–orbit-coupling model.

For thin films, surfaces and interfaces should also influence the spin–orbit-coupling effect as it depends on the local symmetry. Therefore measurements of the FMR at the selected composition $x = 0.7$ of Fe_xCo_{1-x} layers at different thicknesses have been conducted to determine the thickness dependence of the magnetic parameters. For a layer thickness t in the range of 2–20 nm the effective magnetization shows the expected decrease with $1/t$ from which the surface anisotropy and the saturation magnetization can be determined (Pflaum 1995). A most interesting result is the observed thickness dependence of the magneto-crystalline anisotropy field K_1/M (figure 4). K_1/M increases monotonically and nearly linearly with the

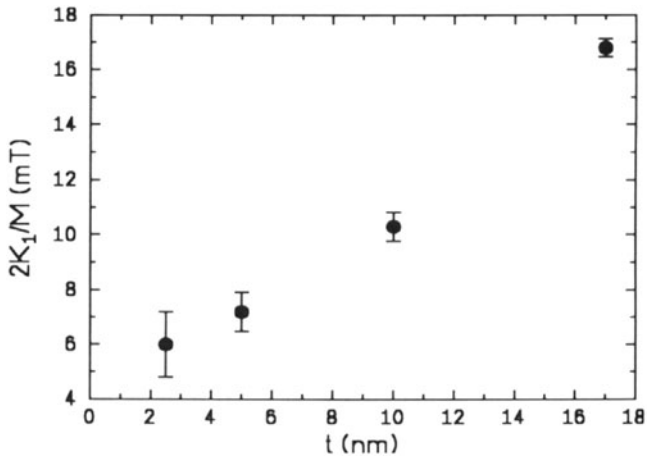

Figure 4. Thickness dependence of the magnetocrystalline anisotropy field $2K_1/M$ in Fe_xCo_{1-x} at room temperature.

thickness of the alloy layer. This thickness dependence is assumed to be responsible for the different concentrations of the crossover of K_1/M in the film and the bulk sample as shown in figure 1. According to the result displayed in figure 4 the zero-crossing is shifted to lower Co concentrations with decreasing layer thickness. The microscopic origin of this shift is most probably changes of the local structure with decreasing thickness. This is supported by the increase of the uniaxial anisotropy with decreasing layer thickness. Also the frequency independent part of the FMR line width is larger for thinner films supporting the arguments. For the intrinsic part and therefore for the Gilbert damping constants the same trend was observed. The G-factor increases by about 50% when the thickness is increased from 2.5 to 15 nm (Pflaum 1995). This increase is attributed to the increased roughness of the thinner alloy layers. For the g-factor within the experimental uncertainty it was not possible to detect a trend when the thickness of the layer was varied.

4.2. Interface induced effects in Co/Cr(100)

With regard to the influence of the local symmetry on the spin–orbit effect the system Co/Cr(001) offers a further aspect. Co which has hcp structure in bulk samples can be arranged in an fcc lattice if it is grown on Cu or on MgO as shown in the previous chapter. On a suitable substrate, on the other hand, Co may be forced to grow in the bcc phase as demonstrated by Prinz (1985) for Co on GaAs. Although As diffusion was probably important to stabilize the cubic phase of Co on GaAs for Co grown on Cr(001) reported here at least an incipient transition to the bcc phase could be observed which is accompanied by a remarkable change of the g-factor of Co.

Thin epitaxial films of Co were grown by molecular beam epitaxy (MBE) on Cr(001). The substrate was $Al_2O_3(1\bar{1}02)$ with a buffer layer of Nb(001) (Donner 1994). The structural analysis of these films shows that Co grows in hcp phase with the c-axis aligned parallel to the Cr(110) axis (Metoki *et al* 1994). For a small layer thickness Co tries to adapt to the Cr(001) plane with a large deformation along the normal of the plane which exceeds considerably the Poisson ratio. This deformation is accompanied by a continuous transition from hcp phase to a bcc phase which, however, is reached only asymptotically as demonstrated by the thickness dependence of the x-ray diffraction intensity of the hcp peak (figure 5).

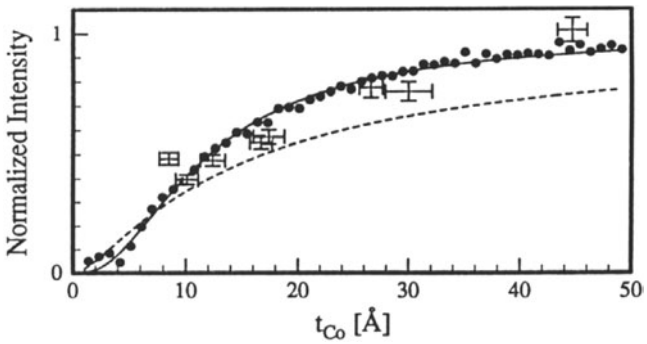

Figure 5. Intensity of the hcp{11.1} spot as a function of the Co layer thickness in Co/Cr(001) (Donner 1994).

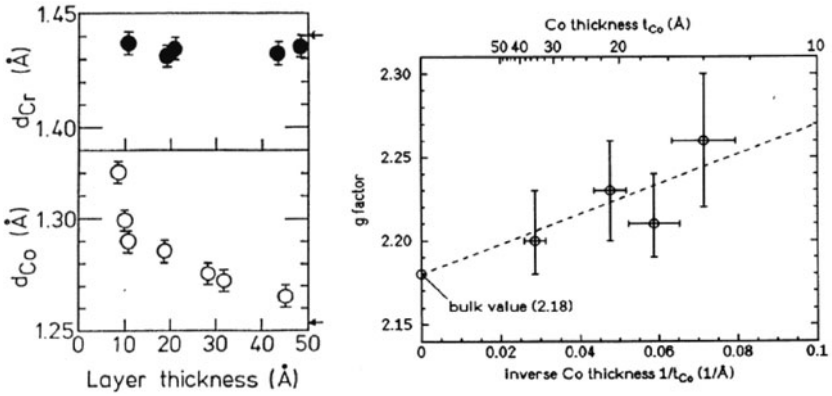

Figure 6. Layer thickness dependence of the in-plane lattice constants of Co and Cr (left). g-factor of Co/Cr(001) layers as a function of the inverse Co layer thickness (right).

Angle and frequency dependent FMR measurements were performed to determine anisotropy fields, g-factor and the Gilbert damping constant (Schreiber 1995). A particular feature is the appearance of two critical thicknesses for the out-off-plane anisotropy which define the change of the sign of the magnetization and the change of the orientation from in-plane to perpendicular to the plane. The Co film also exhibits a large surface anisotropy which is partially accounted for by the magneto-elastic interaction with the substrate.

The g-factor for layers of different thickness increases with decreasing layer thickness (figure 6). This decrease which obeys a $1/t$ law is directly correlated with the elongation of the Co lattice perpendicular to the plane. The g-factor of the thinnest film is 2.26 and corresponds to an orbital contribution of about 13%. Bulk hcp Co has a g-factor $g = 2.18$ corresponding to 9% orbital contribution. The line width of the FMR of Co/Cr(001) is dominated by the inhomogeneous part which essentially reflects the large impact of the magneto-elastic deformations which is inhomogeneously distributed across the film. Due to the high anisotropy values there is a considerable variation of the resonance in the plane which contributes to the static line width. Although the intrinsic line width could be deduced for some layer thickness due to the large error bars of these data we could not establish a correlation between g-factor and Gilbert damping constant.

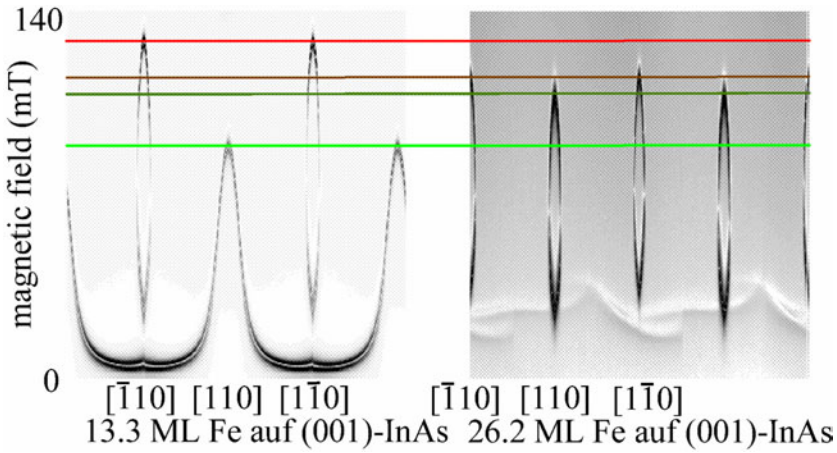

Figure 7. Angle dependence of the FMR field of Fe/InAs(001) for two different Fe-layer thicknesses below and above the thickness where the structural relaxation occurs.

4.3. Structural relaxation induced effects in Fe/InAs(001)

Structural relaxation can occur in epitaxially grown films in order to minimize the elastic energy caused by the lattice mismatch between film and substrate. The relaxation of the lattice is accompanied by the generation of extended lattice defects such as dislocation planes and starts at a certain number of monolayers (ML). As the local order is changed in the course of this process a marked influence on the spin–orbit coupling effects is also expected. On InAs(001) Fe starts to grow as ellipsoidal islands of which the orientation is determined by the reconstruction of the In-terminated surface (Berse 2002). The long axes of the ellipsoids are aligned along the (110) direction. The lattice relaxation occurs at a thickness less than 20 ML.

The in-plane angle dependence of the FMR field provides direct information on the anisotropy changes as a function of the layer thickness (figure 7) (Spoddig 2002, Meckenstock *et al* 2002). From the plots of figure 7 one can easily identify a twofold and a fourfold symmetry. At thicknesses smaller than 20 nm the Fe films exhibit a large in-plane uniaxial anisotropy along the (110) axis of the reconstructed InAs substrate. The cubic magnetocrystalline anisotropy, however, is much smaller compared to the one in bulk iron (table 1). At thicknesses above 20 nm the uniaxial anisotropy nearly vanishes. However, the magnetocrystalline anisotropy increases, approaching a value which is close to that of the bulk material.

All determined values are collected in table 1. The g-factor values were obtained from the frequency dependent measurements which allow a very accurate determination of g by plotting the resonance fields versus the square of the resonance frequency (figure 8). Using this plot the anisotropies do not intervene in the determination of the g-factor. The most surprising result is the observation of an in-plane anisotropy of the g-factor in the structural relaxed films whereas the g-factor of the non-relaxed films is isotropic. The magnitude of the g-factor in the relaxed films is markedly enhanced as compared to the free ion value and to that in the non-relaxed film (table 1).

The surprising new experimental result of an anisotropy dominated effect at small Fe-layer thickness ($<$20 ML) and a magnetic moment anisotropy in the structural relaxed film for thicknesses $>$20 ML is obviously related to particular growth conditions on top of the reconstructed InAs(001) substrate. The considerable lattice mismatch leads to an axial distortion of the Fe lattice and is the origin of the large uniaxial anisotropy at smaller layer

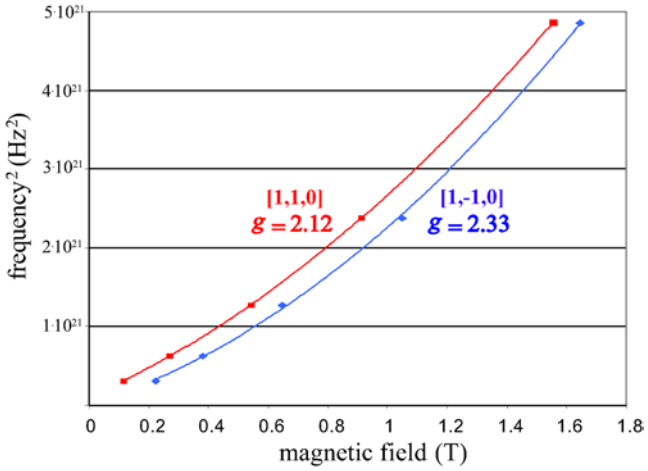

Figure 8. Plot of the resonance frequencies versus the resonance fields of the FMR signal from Fe/InAs(001) for a structural relaxed film. Errors of the measurements are well within the symbol sizes. The full curves are adjusted according to relation (10) (Meckenstock *et al* 2002) and represent the hard and easy directions for the g-factor.

Table 1. Magnetic parameters as a function of Fe thickness in Fe/InAs(100) deduced from frequency and angle dependent FMR at room temperature.

Thickness (nm)	Magnetization (A m^{-1})	Surface anisotropy (J m^{-2})	Crystalline anisotropy (J m^{-3})	Uniaxial anisotropy (J m^{-3})	g-factor (hard axis)	g-factor (easy axis)
0.45			$(0.5 \pm 0.5) \times 10^4$	1.1×10^4	+	+
0.65			1.1×10^4	1.1×10^4	+	+
1.44	1.6×10^6	0.6×10^{-3}	3.7×10^4	1.8×10^4	2.09	2.09
1.91			3.9×10^4	2.0×10^4	2.14	2.15
3.76			4.8×10^4	0.3×10^4	2.33	2.12

thicknesses. The reduced value of the cubic magnetocrystalline anisotropy parameter K_1 is attributed to a tetragonal distortion. In the thicker relaxed films the uniaxial anisotropy vanishes whereas simultaneously the magneto-crystalline anisotropy approaches its bulk value, indicating that the tetragonal distortion has vanished. Instead the g-factor deduced from the FMR data becomes anisotropic with the principal axes oriented parallel and perpendicular to the directions induced by the reconstruction of the InAs surface. The behaviour of the uniaxial and magnetocrystalline anisotropy on one hand and that of the g-factor on the other hand cannot be explained by the same microscopic mechanism. The anisotropies are obviously governed by the elastic strain induced effects which determine their behaviour in the non-relaxed thin films. The influence on the g-factor is too small to be detected within the broad resonance lines, particularly because of the expected anisotropy due the proposed tetragonal distortion. Therefore the local symmetry effects on the spin–orbit coupling cannot be responsible for the observed large anisotropy of the g-factor in the relaxed films. This conclusion is supported by the behaviour of the FMR line width. The intrinsic part of the line width which is proportional to the slope of its frequency dependence does not change in the same way as the g-factor when one goes from the non-relaxed to the relaxed film (figure 9). The observed decrease of both the inhomogeneous contribution to the line width and the slope of its frequency dependence when

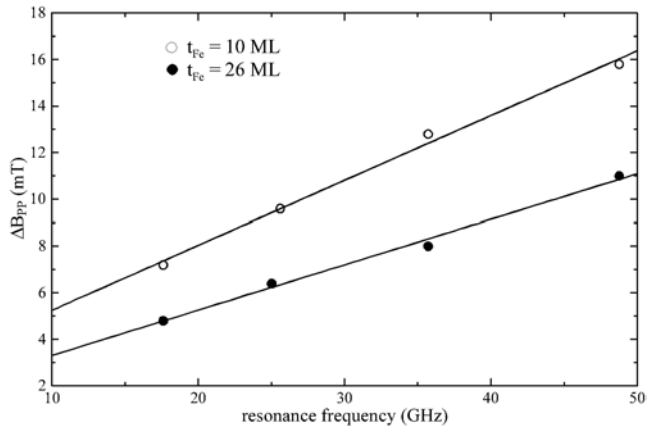

Figure 9. Frequency dependence of the FMR peak to peak line width of Fe/InAs(001) for different layer thicknesses. The magnetic field was aligned along the easy direction of magnetization (Spoddig 2002).

one goes from the non-relaxed to the relaxed film is more likely related to the behaviour of anisotropy fields than to that of the measured g-factor. The origin of the observed anisotropy of the g-factor is still unknown. A possible explanation could be a supplementary contribution to the magnetic moment originating from inner surfaces (Handschuh 1995). Inner surfaces are generated during the structural relaxation of the film as dislocation planes and have to be oriented in one direction in order to compensate the elastic deformation energy perpendicular to the direction of the uniaxial anisotropy caused by the epitaxial growth. As for iron the magnetic moment near the surface is enhanced, this effect explains qualitatively both the increase of the g-factor as well as its in-plane anisotropy.

5. Conclusions

FMR studies of the g-factor and of the Gilbert damping constant provide a powerful tool to investigate spin–orbit effects in magnetically ordered transition metal compounds. In metallic compounds there exists a direct relation between the g-shift and the G-value which can be used to identify the origin of the observed effects. This has been demonstrated for thin films of the alloy system FeCo and for Fe on InAs. In FeCo films the variation with composition of the g-factor and of the Gilbert damping constant have been found to obey the relation predicted in the frame of the model based on the spin–orbit-coupling mechanism. The observed deviations of the measured concentration dependence of the g-factor from the model of two weakly coupled magnetic systems points towards a more complex band structure in the mixed compound. The anisotropy of the measured g-factor observed in structural relaxed Fe on InAs(001), on the other hand, cannot be accounted for by changes of the local symmetry mediated by the spin–orbit coupling mechanism. A possible origin seems to be the additional contribution to the magnetic moment from inner surfaces which are introduced in the course of the structural relaxation. The absence of a detectable correlation between the thickness dependence of the Gilbert damping constant and of g-factor supports this interpretation. Direct evidence of local structural order on the spin–orbit coupling effects provides the g-factor changes in Co layers deposited on Cr(001). With decreasing Co-layer thickness there exists an incipient transition of Co from its hcp phase to a bcc phase which, however, is reached only asymptotically.

With the elongation of the Co lattice perpendicular to the plane when the layer thickness is decreased the g-factor increases linearly with the inverse power of the thickness. Due to the large inhomogeneous contribution to the FMR line width it was not possible to determine the Gilbert damping constant of these films with sufficient accuracy. But qualitatively, G shows an increase with decreasing layer thickness. The magnetocrystalline anisotropy which is governed by the spin–orbit coupling also displays systematic trends which in the cases of the FeCo and Co/Cr systems were consistent with the changes of the g- and G-factors. An analytical relation between the magnetocrystalline anisotropy and the g-factor could not be established. Altogether, the presented experimental results stress the importance of frequency dependent FMR measurements for the investigation of the spin–orbit coupling in magnetically ordered 3d transition metal compounds.

Acknowledgment

This work has been performed in the frame of the Sonderforschungsbereich 491 and 166 and of the Volkswagenstiftung.

References

Abragam A and Bleany B 1970 *Electron Paramagnetic Resonance of Transition Ions* (Oxford: Clarendon)
Anisimov A N, Farle M, Poulopoulos P, Platow W, Baberschke K, Isberg P, Wäppling R, Niklasson A M N and Eriksson O 1999 *Phys. Rev. Lett.* **82** 2390
Berse M 2002 *Master Thesis* Faculty of Astronomy and Physics, Ruhr University Bochum
Bruno P 1989 *Phys. Rev.* B **39** 865
Daalderop G H O, Kelly P J and Schuurmans M F H 1995 *Ultrathin Magnetic Structures* vol 1, ed J A C Bland and B Heinrich (Heidelberg: Springer) p 40
Donner W 1994 *PhD Thesis* Ruhr University Bochum
Eriksson O 2001 *Electronic Structure and Magnetism* ed K Baberschke, M Donath and W Nolting (Berlin: Springer) p 243
Gilbert T L 1955 *Phys. Rev.* **100** 1243
Hall R C 1960 *J. Appl. Phys.* **31** 157S
Handschuh S 1995 *PhD Thesis* University of Cologne
Kambersky V 1970 *Can. J. Phys.* B **26** 2906
Kittel Ch 1949 *Phys. Rev.* **76** 743
Landau L D and Lifschitz E M 1935 *Phys. Z. Sowjetunion* **8** 153
Meckenstock R, Spoddig D, Pelzl J, Berse M, Kneppe M, Köhler U and Frait Z 2002 *Phys. Rev.* B at press
Metoki N, Donner W and Zabel H 1994 *Phys. Rev.* B **49** 17351
Meyer A J and Asch G 1961 *J. Appl. Phys.* **32** 330S
Mühge Th 1994 *Master Thesis* Faculty of Physics and Astronomy, Ruhr University Bochum
Orton J W 1968 *Electron Paramagnetic Resonance* (London: Iliffe)
Pake G E 1962 Paramagnetic resonance *Frontier of Physics* ed D Pines (New York: Benjamin)
Pflaum J 1995 *Master Thesis* Faculty of Physics and Astronomy, Ruhr University Bochum
Pflaum J, Schreiber F, Mühge Th and Pelzl J 1995 *J. Magn. Magn. Mater.* **148** 127
Prinz G A 1985 *Phys. Rev. Lett.* **54** 1051
Schreiber F 1995 *PhD Thesis* Ruhr University Bochum
Schreiber F, Pflaum J, Frait Z, Mühge Th and Pelzl J 1995 *Solid State Commun.* **93** 965
Spoddig D 2002 *PhD Thesis* Ruhr University Bochum
Tsuya N 1952 *Prog. Theor. Phys.* **7** 263
Reck R A and Fry D L 1969 *Phys. Rev.* **184** 492
Ujfalussy B, Szunyogh L, Bruno P and Weinberger P 1995 *Phys. Rev. Lett.* **77** 1805
Van Vleck J H 1950 *Phys. Rev.* **78** 266
Vonsovskii S V 1960 *Ferromagnetic Resonance* (Oxford: Pergamon)
Wangsness R K 1953 *Phys. Rev.* **91** 1085